

# First Real-Time Detection of Ambient Backscatters using Uplink Sounding Reference Signals of a Commercial 4G Smartphone

Ahmed ElSanhoury , Islam Galal, Khaled AlKady, Aml ElKhodary, Ayman M. Hassan 

Dinh-Thuy Phan-Huy , *Senior Member, IEEE*

**Abstract**—Recently, cellular Ambient Backscattering has been proposed for 4G/5G/6G networks. An Ambient backscatter tag broadcasts its message by backscattering ambient downlink waves from the closest base station according to a predefined pattern. A tag is detected by smartphones nearby. This paper presents, for the first time, a novel ambient backscatter communication system exploiting uplink ambient waves from smartphones instead of downlink waves. In this novel system, the base station connected to a smartphone monitors the uplink pilot signals and detects tags in proximity. The proposed system is implemented and tested with prototypes of tags, a commercial 4G smartphone and a 4G Software Defined Radio base station. At the base station side, a non-coherent correlator receiver is implemented, and a novel technique based on pre-correlation data processing is proposed to separate useful variations on pilot signals due to tags from variations due to time varying channel effects. To deal with collision between multiple tags, distinct Gold pseudo noise codes with minimum cross correlation are used. Tests are run in different indoor and outdoor environments. A receiver detection probability of 95% has been achieved at 0.5% False-alarm probability when the tag is at 5 meters from the UE. At the refresh rate of 2 seconds, the proposed scheme is suitable for tracking objects at moderate speeds and can therefore be used for many passive IoT-based applications.

**Index Terms**— LTE, Uplink, Sounding Reference Signals, Backscatter Communication, Tag Detection, Wireless Communication, IoT, Zero Energy Device.

This work is in part supported by the European Project Hexa-X II under (grant 101095759). (*Corresponding author: Ahmed ElSanhoury*)

Ahmed ElSanhoury is with Orange Innovation Centre, Orange Egypt, Giza, 12578 Egypt (e-mail: [ahmed.elsanhoury@orange.com](mailto:ahmed.elsanhoury@orange.com)).

Islam Galal is with Orange Innovation Centre, Orange Egypt, Giza, 12578 Egypt (e-mail: [islam.galal@orange.com](mailto:islam.galal@orange.com)).

Khaled Alkady is with Orange Innovation Centre, Orange Egypt, Giza, 12578 Egypt (e-mail: [khaled.alkady@orange.com](mailto:khaled.alkady@orange.com)).

Aml ElKhodary is with Orange Innovation Centre, Orange Egypt, Giza, 12578 Egypt (e-mail: [aml.elkhodary.ext@orange.com](mailto:aml.elkhodary.ext@orange.com)).

Ayman M. Hassan is with the Department of Electrical Engineering, Benha University, Benha, Al-Qalyubia 6470015 Egypt, and also with Orange Innovation Centre, Orange Egypt, Giza, 12578 Egypt (e-mail: [ayman.mohamed@bhit.bu.edu.eg](mailto:ayman.mohamed@bhit.bu.edu.eg), [ayman.hassan@orange.com](mailto:ayman.hassan@orange.com)).

Dinh-Thuy Phan-Huy is with Networks Department, Orange Innovation, Châtillon, Paris, 92356 France (e-mail: [dinhthuy.phanhuy@orange.com](mailto:dinhthuy.phanhuy@orange.com)).

## I. INTRODUCTION

Ambient backscatter communication (AmBackCom) has become a promising technology for low-power, low-cost wireless communication, especially in the context of Internet of Things (IoT) applications. This field has gotten significant advancements in recent years, with researchers exploring various aspects of the technology across different communication protocols and scenarios. [1]

AmBackCom is based on passive reflection and modulation of an incident radiofrequency (RF) wave. By using these reflections in a predetermined sequence, the receiver could receive the message that is being sent from the backscatter device.

Backscatter communication, especially ambient signal based on backscatter is a promising future for Internet of Things (IoT) devices. Recently, researchers proposed the systems to utilize different existing signals like Wi-Fi, Bluetooth, Zigbee, and LoRa for backscatter communication. [2][3]

The foundational work in the domain of ambient backscattering was presented by Liu et al. (2013) [4], in which the concept of ambient backscatter communication was introduced. Their research demonstrated the feasibility of wireless communication using existing radio frequency (RF) signals, without the need for dedicated power sources or transmitters. This revolutionary work paved the way for subsequent research in the field.

For example, the first system uses the Wi-Fi signals to carry backscatter data published in [5]. From HitchHike [SenSys'16] to MOXcatter in [MobiSys'18], the Wi-Fi signal-based backscatter systems were improved to support newer Wi-Fi protocols like OFDM and MIMO signals, [6] & [7] respectively. All of this research in addition to BackFi (SIGCOMM 2015) [7] and FreeRider (CoNEXT 2017) [8] investigated the use of Wi-Fi signals for backscatter communication, demonstrating the potential for leveraging ubiquitous Wi-Fi infrastructure for IoT connectivity.

The scalability and practical implementation of ambient backscatter systems have also been a focus of recent research. Zhao et al. (2018) proposed X-tandem, a system for multi-hop backscatter communication using commodity Wi-Fi, addressing the limited range of traditional backscatter systems [9].

Interscatter [SIGCOMM'16] [10] and FreeRider

> REPLACE THIS LINE WITH YOUR MANUSCRIPT ID NUMBER (DOUBLE-CLICK HERE TO EDIT) <

[CoNEXT'17] [8] were proposed to use Bluetooth signal and FreeRider can support zigbee signal as well. Consequently, several systems were developed to use the newer IoT protocol such as LoRa. Talla et al. (2017) demonstrated the feasibility of LoRa backscatter for long-range, low-power communication [11]. Hesar et al. (2019) [12] introduced NetScatter [NSDI'19], a system enabling large-scale backscatter networks, further enhancing the scalability of the LoRa technology rather than LoRa Backscatter [IMWUT'17] [11], and PLoRa [SIGCOMM'18] [13]. Similarly, Wang et al. (2017) explored the use of FM radio signals for backscatter communication in urban environments and smart textiles [14].

However, there're critics that say the above signals are not excellent carriers for backscattering because of the limited coverage in space and time domains. In space domain for example, mobile networks have much wider coverage across the country or even the world. [15] has proposed to introduce ambient backscatters in mobile networks, to provide asset-tracking service. On the other hand, in the time domain, the traditional backscattering techniques could fail due to intermittent traffic patterns and shelled channels. On the contrary, the continuous LTE signal allows reliable backscatter communication. Effort toward LTE DL direction was made in [16] and [17] where the downlink cell specific reference signals and pilots are used. This work concerns LTE UL direction and realizes the concept discussed in [18].

3GPP considers a new work item related to backscattering in Rel.18 and Rel.19 under Ambient IoT keyword through two 3GPP specifications 38.848 [19] and 22.840 [20] of RAN group and System aspects group, respectively. Moreover, an initial version of the study 3GPP document 38.769 [21] on solutions for Ambient IoT (Internet of Things) in NR was drafted recently in November. The road towards 6G means that a broad range of small communication devices M2M and its applications will be used.

Three levels of taxonomies are introduced in the referred 3GPP documents: device types, connectivity topologies, and deployment scenarios. Multiple dedicated channels are articulated in the standard to realize those different topologies and deployment scenarios. Dedicated channels like continuous wave to device (CW2D), device to reader (D2R), and reader to device (R2D) are introduced.

This work aims at realizing, for the first time, a backscattering communication to be piggybacked on the uplink direction of LTE signal without needs of a dedicated CW2D source. This goal has a great business impact as the realization could deal with the conventional UEs (COTS) as it's without any changes. Also, it removes any need for base-station hardware changes. As it moves all required changes in base-station to be software only. The work realized the backscatter communication using the sounding reference signal, SRS. It's important to note that the 3GPP standard - so far - is not considered the reference signals in realizing D2R channel communication including demodulation reference signal (DMRS), phase-tracking reference signal (PTRS), and sounding reference signal (SRS).

The following sections are organized to represent the details of this work. The following section describes the system architecture end to end to give an overview of the idea. In the third section, the detection technique at the reader (in our case, it's the base-station) of the backscattering device (BD) or tag is explained. Multiple tags could be identified using the algorithm that demonstrated in the fourth section. To enhance the process of the tags identification and to overcome wireless channel variations, some signal processing methods are demonstrated in the fifth section. Finally, experimentation results are revealed followed by the conclusion in the sixth and the seventh section, respectively.

## II. SYSTEM DESCRIPTION

The system architecture for tag detection using SRS in UL LTE could be described as the following three main items as shown in Fig.1: UE (i.e. assisting node), Tag (i.e. BD), and Base-station (i.e. reader). The ambient signal here is considered the LTE system (could be NR as well). The system is using UE as a COTS, commercial on the shelf user equipment. In the attach procedure (i.e. 5 messages), the SRS common configuration is used to configure the UE to send SRS signals according to the common configuration in the standard.

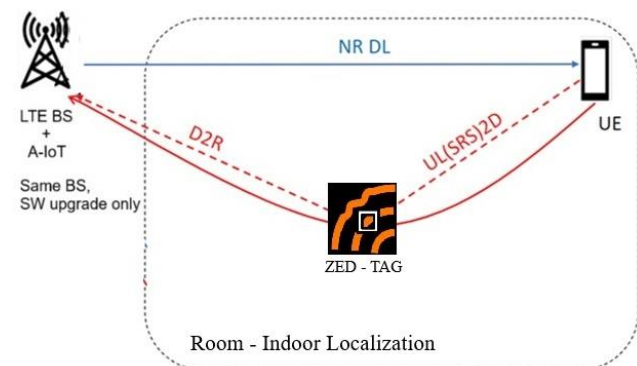


Fig. 1. System Architecture of Tag Detection using SRS in UL

The periodicity and the bandwidth of SRS are determined in this configuration. That means that the UE is commanded to send in its UL frames a pre-configured SRS regardless of a voice service session that's normal usage of SRS signal in VoLTE service. The SRS is transmitted at the last symbol of UL slot. The SRS configuration is notified to the UE by a couple of RRC messages. Common RRC messages carrying SRS configuration information could be sent in one of the following messages: SIB2, RRC connection setup, or RRC connection reconfiguration. In the initialization phase (eNB commands UE): Setting up the SRS signal requires: *srs-BandwidthConfig*, and *srs-SubframeConfig* [22]. Also, it is called Cell specific SRS configuration which defines the subframes that can contain SRS transmissions as well as the set of SRS bandwidths available in the cell as depicted in Fig.2.

> REPLACE THIS LINE WITH YOUR MANUSCRIPT ID NUMBER (DOUBLE-CLICK HERE TO EDIT) <

```
eNB broadcasts RRC (36.331) SystemInformationBlockType2
SoundingRS-UL-ConfigCommon ::= CHOICE {
  release NULL,
  setup SEQUENCE {
    srs-BandwidthConfig ENUMERATED {bw0, bw1, bw2, bw3, bw4, bw5, bw6, bw7},
    srs-SubframeConfig ENUMERATED {sc0, sc1, sc2, sc3, sc4, sc5, sc6, sc7, sc8, sc9, sc10, sc11, sc12, sc13, sc14, sc15},
    ackNackSRS-SimultaneousTransmission BOOLEAN,
    srs-MaxTxPts ENUMERATED {true} OPTIONAL -- Cond TD0
  }
}
```

Fig. 2. Cell Specific or Common SRS Configuration in SIB2

The base-station and the core network in that work were based on the srsRAN open source as depicted in the Fig.3.

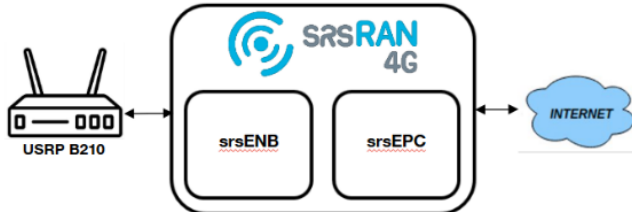


Fig. 3. srsRAN using USRP B210, [23]

### III. TAG DETECTION

In 4G networks, The SRS (Sounding Reference Signal) is a reference signal used to give the base station estimate of the uplink channel characteristics. This signal is sent in the UP-Link from the UE to the Base Station. UE can transmit the SRS signal every 2 subframes at the most and every 320 subframe at the least. In our case, the SRS is sent periodically every 10ms and *srs-BandwidthConfig* is 0. That means 48 physical resource block is occupied and odd or even subcarriers are selected. This will lead to the length of each SRS is  $(48/2 \times 12/2) = 144$  complex number which represents the number of sub-carriers assigned for SRS signal received in one subframe. The signal flow of the whole detection process is illustrated in the Fig.4.

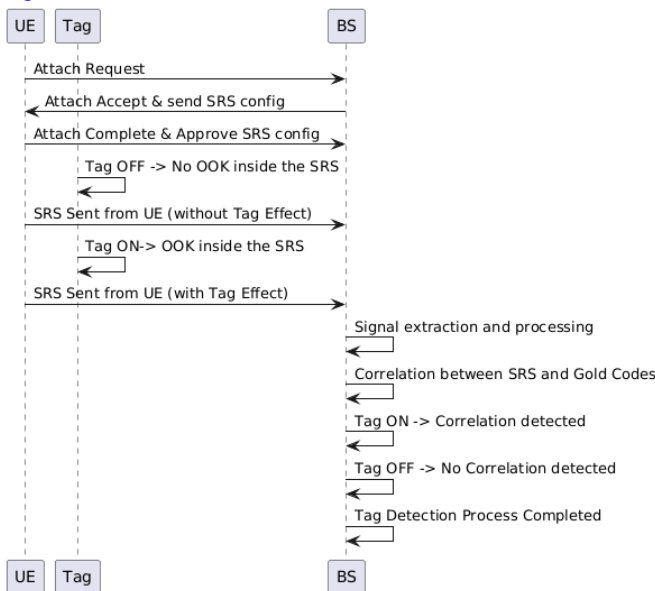


Fig. 4. Signal Flow of Tag Detection

The SRS signal is a Zadoff-Chu sequence. The sequence is extracted in the form of an array of complex floats. One of the key properties of the Zadoff-Chu sequence is that it has a

constant magnitude. The Fig.5 shows Zadoff-Chu sequence of each SRS and the average magnitude of each SRS signal.

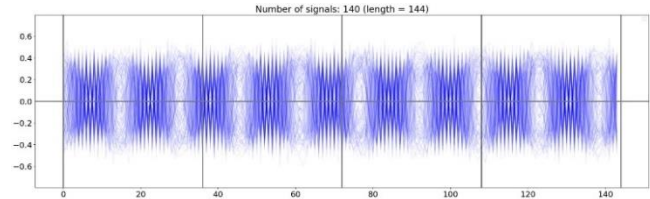


Fig. 5. Zadoff-Chu Sequence of 140 Signals

The graph in the Fig.6 is constructed by calculating the mean of the magnitude of each element in the vector that has length of 144 complex elements as described in the beginning of this section. Each point in the graph represents that value of that mean. It could be noticed that the mean of 144 magnitude elements maintains a constant value when tag is off with minor deviations only due to surrounding external effects.

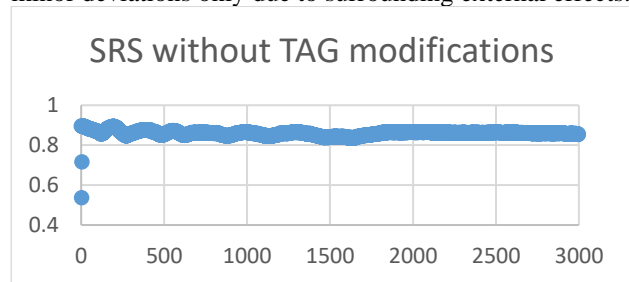


Fig. 6. Average Magnitude of the SRS Signal

A bunch of SRS signals (3000 samples) received in multiple LTE frames were examined by the same mentioned calculation to construct the graph. When the tag is turned on, the calculated average value is affected by the tag RF switch state as shown in the Fig.7 Hence, the tag existence could be detected.

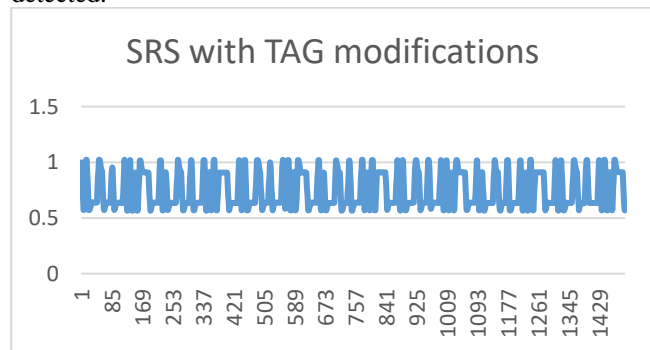


Fig. 7. Tag Modifications Effect on the SRS Signal

### IV. TAG IDENTIFICATION

Once the SRS is extracted at the receiver every 10ms, it is used for tag identification. During this process, if the tag is off and the channel is assumed to be stationary, the SRS maintains a nearly constant amplitude. However, when the tag is on, the SRS amplitude varies according to the Gold Code pre-installed on the tag.

Correlation analysis is then performed between the received SRS signal and the set of available Gold Codes while the tag is active. If the correlation value exceeds a predefined

> REPLACE THIS LINE WITH YOUR MANUSCRIPT ID NUMBER (DOUBLE-CLICK HERE TO EDIT) <

threshold—indicating a high positive or negative correlation—the tag ID is accurately identified. The block diagram of the whole process of the tag identification is depicted in the Fig.8.

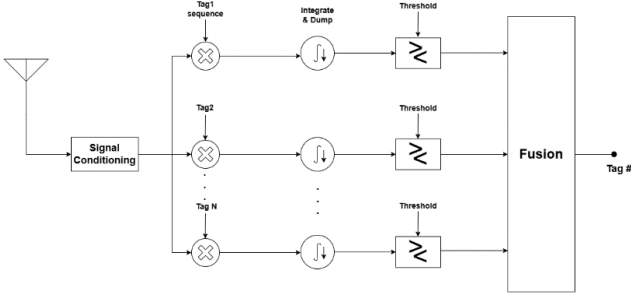


Fig. 8. Tag Identification Block Diagram

The goal in the tag identification is to reliably detect the correct tag by correlating with the specified Gold Code from among all available codes, aiming to maximize detection accuracy with minimal misdetection and nearly zero false alarms. The autocorrelation versus the cross-correlation graph for specific tag identification is drawn in the Fig.9.

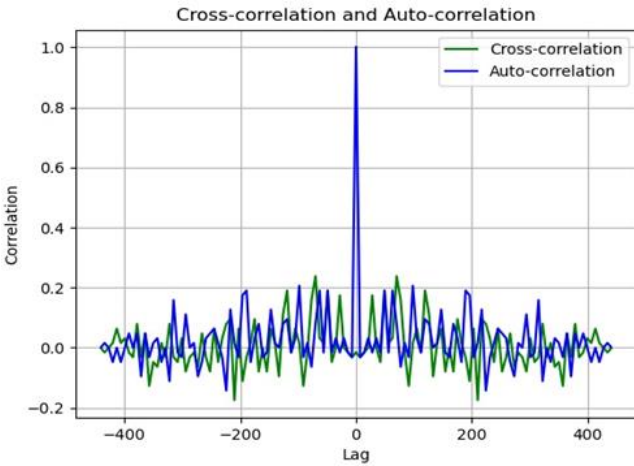


Fig. 9. Autocorrelation versus Cross-correlation

Each tag is identified using a unique Gold Code. Gold Codes are generated by XORing two m-sequences with specific characteristics, using preferred polynomials. The advantage of using Gold Codes lies in their ability to minimize cross-correlation while maximizing autocorrelation, as illustrated in the graph. Each Gold Code is pre-installed on the tag, and correlation analysis is performed between this code and the extracted SRS when the tag is active. These codes are derived from maximum-length sequences (m-sequences) generated by linear feedback shift registers (LFSRs). By XORing these sequences, we obtain distinct Gold Codes with desirable properties: low cross-correlation, strong autocorrelation, efficient generation using two LFSRs, resistance to interference, and a large set of unique codes. These attributes enable us to distinguish between different Gold Codes, each pre-installed on a unique backscattering tag. The preferred used polynomials of 31 length gold sequence:

- $x^5 + x^2 + 1$  (1)

- $x^5 + x^4 + x^3 + x^2 + 1$  (2)

while the preferred used polynomials of 63 length gold sequence:

- $x^6 + x + 1$  (3)

- $x^6 + x^5 + x^2 + x + 1$  (4)

## V. SIGNAL PROCESSING

The Signal Processing section includes all the modifications that has been implemented on the sounding reference signal to solve any problems that have been appeared in the SRS after the extraction of it due to the channel effects, the fading and all the fluctuations that may have effect on the SRS. These interruptions make the correlation score decreases, so it effects on the tag identification. Signal Processing Techniques include calculating the average magnitude of the signal, after that there are the filtrations that have been applied on the SRS and finally the correlation between the SRS and the Set of Gold Codes. This comprehensive approach enhances the overall reliability of the system, as illustrated in the following graph at the Fig.10.

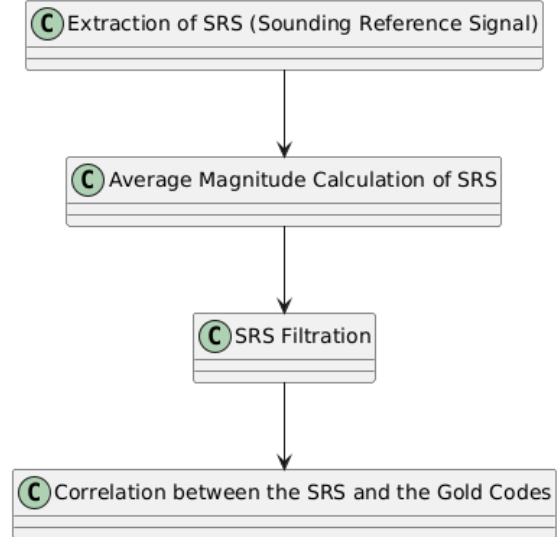


Fig. 10. Signal Processing for Tag Identification

### A. Average Magnitude Calculation of SRS

After Sounding Reference Signal is extracted, which consists of 144 complex number. The magnitude of each complex number is calculated by the following formula:

$$|SRS_n| = \sqrt{(\text{Re}(SRS_n))^2 + (\text{Im}(SRS_n))^2} \quad (5)$$

where  $|SRS_n|$  is the magnitude of each complex number, and  $n = 1, 2, \dots, 144$ . Next, the average magnitude of these 144 complex numbers is computed to obtain a single representative value for the SRS. This average is calculated using the following equation:

$$A = \frac{1}{M_{sc}} \sum_{n=1}^{M_{sc}} (|SRS_n|) \quad (6)$$

where  $A$  is the average of SRS each 10ms.



> REPLACE THIS LINE WITH YOUR MANUSCRIPT ID NUMBER (DOUBLE-CLICK HERE TO EDIT) <

### B. SRS Filtration

After calculating the average magnitude of the Sounding Reference Signal (SRS), necessary filters are applied to reduce noise and manage outliers. The SRS Filtration Process begins with a hard-limiting step, which constrains the SRS within specified minimum and maximum values, representing valid signal levels. If the average magnitude falls below the minimum limit, it indicates that the signal was not received. Conversely, if it exceeds the maximum limit, this suggests the signal has been affected by noise or fading. Hard limiting effectively detects most valid SRS values.

Following hard limiting, a median filter is applied to smooth the signal and further reduce noise. This step significantly improves tag detection by mitigating noise introduced through channel effects. Outliers in the signal, which can also impact tag detection and correlation scores, are managed using a standard deviation filter. Since standard deviation measures how much the SRS deviates from its mean, a low standard deviation indicates that the SRS is close to the mean, while a high standard deviation identifies a potential outlier. To address this, outliers are replaced with the mean signal value, ensuring that the filter order does not exceed the repetition period of the Gold Codes.

After filtration, the SRS is prepared for correlation analysis to detect the influence of the backscattering tag on the signal. Let's now review each implemented filter in detail.

### C. Median Filter

The median filter utilizes a circular buffer with a size equal to the order of the filter. Each new SRS signal, extracted every 10ms, is inserted into this buffer. The buffer is then sorted to enable direct access to the median value. Let the buffer be represented as  $x = \{x_1, x_2, x_3, \dots, x_n\}$ , where  $n$  is the filter order. For an odd  $n$ , the median is calculated as:

$$X_{\text{median}} = x\left(\frac{n+1}{2}\right) \quad (7)$$

The implementation of the median filter begins by adding the new SRS value to the circular buffer, which has a size corresponding to the filter order. After inserting the new value, the buffer containing the average magnitudes of the SRS is sorted. Finally, the median element of the sorted buffer is returned.

### D. Standard Deviation Outlier Filter

This filter identifies outliers by checking whether the difference between the signal and the mean exceeds a specified outlier threshold, calculated using the following formula:

$$\text{Outlier Threshold} = \text{Deviation Factor} * \text{Standard Deviation}$$

If the absolute difference exceeds this threshold, the signal is classified as an outlier, and the current value is replaced with the mean. Conversely, if the difference does not exceed the threshold, the original value is retained.

The implementation begins by calculating the mean, which represents the average of the buffer containing SRS signals with a size equal to the filter order. Next, the standard deviation is computed, indicating how much the SRS values deviate from the mean. Finally, the condition is checked:

If  $\text{abs}(\text{current value} - \text{mean}) > \text{outlier threshold}$

then replace the current value with the mean value

If the condition is not met, the current value remains unchanged.

### E. Correlation between SRS and the gold codes

Correlation is the method used to verify the relationship between the Gold Codes and the Sounding Reference Signal (SRS), which is influenced by the backscattering tag. If the correlation values exceed the predefined correlation threshold, this indicates successful correlation and tag detection.

Three types of correlation coefficient calculations are employed: Pearson, Spearman, and Kendall [24]. Pearson's coefficient measures linear correlation, while Spearman and Kendall coefficients focus on comparing the ranks of the data.

#### Pearson's Correlation Coefficient

It is calculated using the following formula:

$$r = \frac{\sum_1^n (x_i - \bar{x})(y_i - \bar{y})}{\sqrt{\sum_1^n (x_i - \bar{x})^2 \sum_1^n (y_i - \bar{y})^2}} \quad (8)$$

Where:

- $x_i$  represents the received SRS values,
- $y_i$  represents the Gold Code sequence,
- $\bar{x}$  and  $\bar{y}$  are the mean values of  $x$ (SRS) and  $y$  (Gold Code), respectively, and
- $n$  is the sequence length.

#### Spearman's Correlation Coefficient

It follows a similar approach to Pearson's but utilizes the ranks of the values instead of their actual magnitudes.

#### Kendall's Correlation Coefficient

It examines pair of observations  $(x_i, y_i)$  and  $(x_j, y_j)$  with  $i < j$ , calculated using the formula:

$$\tau = \frac{(n^+ - n^-)}{\sqrt{(n^+ + n^- + n^x)(n^+ + n^- + n^y)}} \quad (9)$$

After implementing the above three methods, it turned out that Pearson's correlation coefficient is the fastest among the three algorithms. Therefore, we employed Pearson's method for tag detection. The following flow chart at the [Fig.11](#) is showing the implementation of the signal processing starting the signal is extracted until the correlation is done.

## VI. EXPERIMENTATION

This section describes the experiments conducted to verify the identification of the backscattering tags and to ensure that the correlation score and percentage of correlation are high and consistent. The experiment setup consists of three main parts:

- User Equipment (UE): Sends the Sounding Reference Signal (SRS) to the Base Station (BS) to enable it to estimate channel quality.
- Backscattering Device (TAG): Modifies the SRS
- Base Station (BS): Connects with srsRAN 4G project.

> REPLACE THIS LINE WITH YOUR MANUSCRIPT ID NUMBER (DOUBLE-CLICK HERE TO EDIT) <

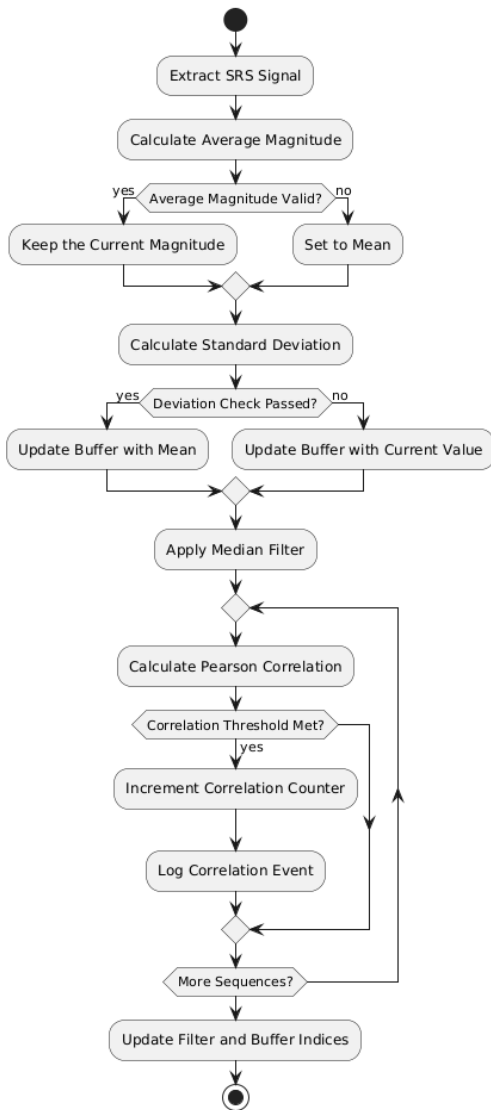


**Fig. 11.** Detailed Signal Processing for Tag Identification

The experiments were implemented in two setups: Indoor Setup and Outdoor Setup. We will describe these setups in the subsections below.

#### A. Indoor Testing

The indoor setup was conducted for two scenarios:

##### First Scenario

This scenario took place in a controlled environment inside a room, with a maximum distance of up to 7 meters between the Base Station (BS) and the tag with User Equipment (UE). The distance between the TAG and UE was maintained at 1 meter.

##### Second Scenario

This scenario involved a longer distance of up to 20 meters. The testing area included obstacles and walls, which introduced significant fading; however, the percentage of correlation detection reached up to 95%, with the distance between the UE and TAG extending to 5 meters.

The tag detection was tested across various positions, orientations, and distances. The results were promising, as

both the correlation score and tag detection remained consistent with each new position and orientation of the UE and the TAG. The setup consisted of the following components as shown in the following graph at the [Fig.12](#):

- USRP: Connects to a laptop running srsRAN software.
- Duplexer: Band 13 (DCM751-782-10A1), operating on Band 13 frequencies.
- Antenna: DeLOCK 88571 antenna (3 dBi).
- Bandpass Filter: Operating in the range of 768-795 MHz.
- COTS UE: Samsung S8.
- Backscattering Tag.

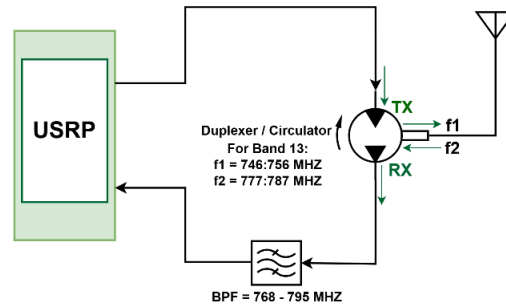


**Fig. 12.** The in-lab setup block diagram

The controlled environment in the first scenario validates the system's ability to maintain a strong correlation between the Sounding Reference Signal (SRS) and the gold code under varying orientations of the User Equipment (UE) at close distances. The objective was to ensure correlation consistency despite changes in UE positioning and Line-of-Sight (LOS) conditions with the TAG and Base Station. The results indicated that the correlation and TAG detection across all positions exceeded 90%. The following Table shows the correlation detection and false alarm.

Orientation	Detection	False Alarm
LOS	98.83%	0.00%
Non-LOS	92.17%	0.00%

The long-distance indoor environment in the second scenario verifies the correlation score at greater distances between the User Equipment (UE) and the TAG, as well as between the TAG and the Base Station. The correlation performance remained consistent up to 5 meters, with only slight variations in the detection percentage. Additionally, the test aimed to evaluate how different positions and distances affected tag detection. The following graph at the [Fig.13](#) illustrates the correlation detection across various distances between the User Equipment (UE) and the TAG, tested under both Line-of-Sight (LOS) and Non-Line-of-Sight (NLOS) conditions between the UE and the Base Station (BS). The [Fig.13](#) demonstrates that the cross correlation and tag detection rates are mostly above 80%, particularly when the distance between the TAG and the User Equipment (UE) is within the range of 1 to 4 meters. Beyond this distance, the correlation and tag detection scores

> REPLACE THIS LINE WITH YOUR MANUSCRIPT ID NUMBER (DOUBLE-CLICK HERE TO EDIT) <

begin to decline. All the experiments are done for a fixed number of sequences equal to 300 sequences. The TAG Detection happens with the different gold codes with different lengths while most time of the experiments done with gold code length 31, each bit of the gold code repeated for 7 times so the total length was  $31*7$  which is 217 and each bit is according to 1 SRS signal which is sent every 10ms so the time of 1 sequence is  $217*10*10^{-3} = 2.17$  seconds. So, to obtain total time of each experiment it will equal to time of one sequence multiplied by total number of sequences =  $2.17*300 = 651$  seconds = 10.85 minutes and total number of SRS signals which is extracted every 10 ms is 10.85 is calculated according to the following formula:

$$\text{Total No of signals} = \frac{\text{Total Time}}{\text{Time of one signal}} = \frac{10.85 \text{ minutes}}{10 \text{ ms}} = \frac{10.85*60*1000 \text{ ms}}{10 \text{ ms}} = 65100 \text{ SRSs} \quad (10)$$

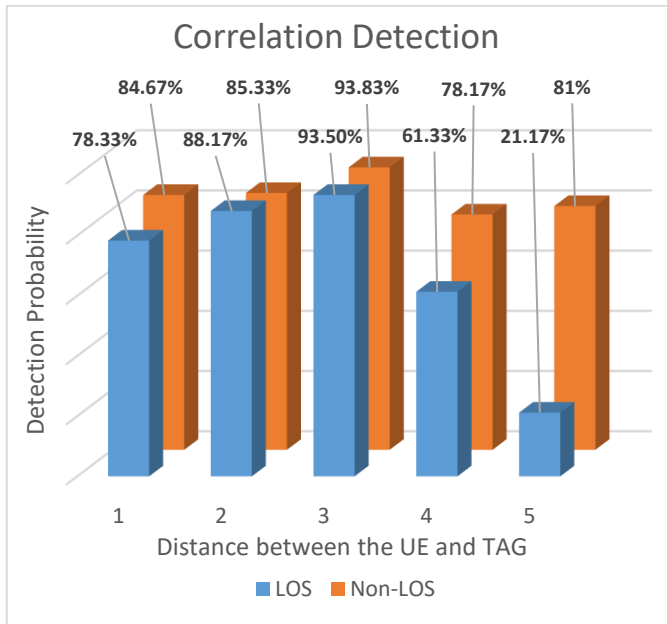


Fig. 13. Tag Detection Results

There are two types of observed false alarms:

- a) Cross False Alarm: This occurs when the TAG is powered ON but is detected with a gold code that is not pre-installed on the specified TAG. The results indicate that this type of false alarm does not exceed 1%, as shown in the table while the distance reaches up to 5 meters.

TABLE II

CROSS FALSE ALARM RESULTS VS ORIENTATION

UE & Tag distance in m	Cross False Alarm	
	LOS	Non-LOS
1	0.5%	0.00%
2	0.00%	0.00%
3	0.00%	0.00%
4	0.33%	0.5%
5	0.67%	1%

- b) False Alarm: This happens when there is no TAG powered ON, yet tag detection or correlation is falsely reported.

This type of false alarm has a detection rate like that of the cross false alarm, generally averaging around 0%, with rare instances where it slightly increases but still does not exceed 1%.

### B. Outdoor Testing

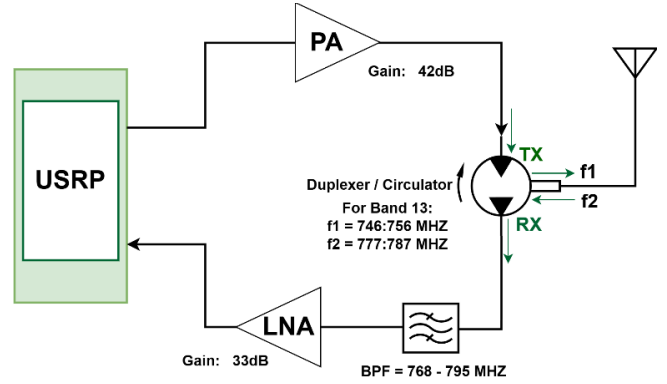


Fig. 14. The Outdoor Testing Block Diagram using RF chain

The goal of the Outdoor Setup is to achieve a longer distance between the base station and the User Equipment (UE) with the TAG while ensuring a stable connection. This setup aims to confirm that TAG Detection can be successfully performed in a real outdoor environment, even under challenging conditions. The distance was extended to 60 meters in both Line of Sight (LOS) and non-Line of Sight (NLOS) scenarios. TAG Detection was successful, although the correlation scores slightly decreased due to channel conditions. To enhance the distance for outdoor testing, a 24V power amplifier and a 12V Low Noise Amplifier were added to the hardware setup as shown block diagram in Fig.14. The implementation of that block diagram is depicted in the outdoor testbed as shown in the Fig.15.

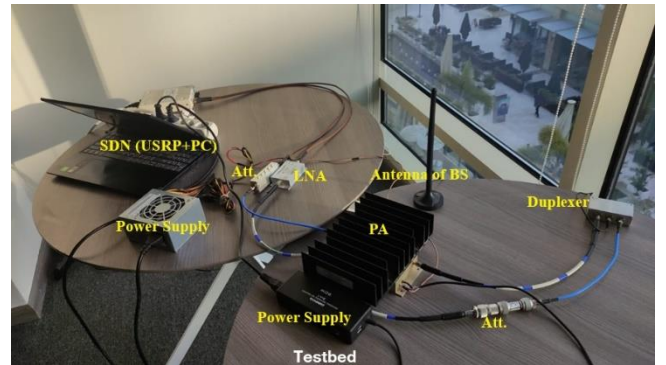


Fig. 15. The Outdoor Testbed Setup

The testbed setup in the Fig.15 is achieved using RF chain as mentioned above that contains from the left: software of core and access network, USRP as SDR element, a transmitter path (Power amplifier), a receiver path (LNA), a duplexer and an antenna in addition to the necessary power supplier elements.

The following photos at the Fig.16 shows the achieved outdoor distance between the eNodeB and the UE with the TAG which reached up to 60 meters.



> REPLACE THIS LINE WITH YOUR MANUSCRIPT ID NUMBER (DOUBLE-CLICK HERE TO EDIT) <

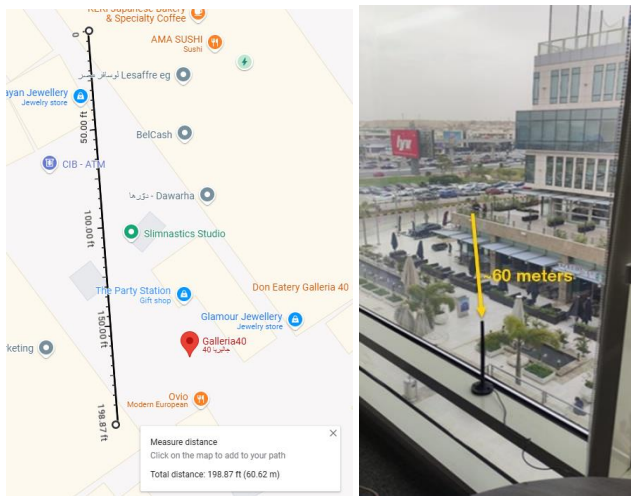


**Fig. 16.** The Outdoor distance between Tag and eNodeB

## VII. CONCLUSION AND FUTURE WORK

A novel backscattering communication technique is presented and proved experimentally. A backscattering device (BD) is able to communicate with its reader (LTE base-station) piggybacked on the LTE uplink signal using COTS UE. Through the sounding reference signal (SRS), the COTS UE is commanded and configured during its attach procedure to send SRS regularly. SRS's signal which is based on Zadoff-Chu sequence (i.e. magnitude equal one) is exploited to reflect the effect of the pseudo noise pattern generated by the BD when the magnitude of the SRS differs from one.

Practical indoor/outdoor experiments were conducted to prove the proposed technique. The experiment shows successful BD communication with promising detection capability for different tag IDs. A detection probability of 95% has been achieved at 0.5% False-alarm probability when the tag is at 5 meters from the UE.

Future work has to be continued to enhance the detection parameters and to overcome the variations of the channel coefficient. An improvement of signal detection, channel estimation, and interference mitigation could be investigated using AI-empowered techniques discussed in literature [25].

## REFERENCES

- [1] Van Huynh, Nguyen, et al. "Ambient backscatter communications: A contemporary survey." *IEEE Communications surveys & tutorials* 20.4 (2018): 2889-2922.
- [2] Wu, Weiqi, et al. "A survey on ambient backscatter communications: Principles, systems, applications, and challenges." *Computer Networks* (2022): 109235.
- [3] Jiang, T., Zhang, Y., Ma, W., Peng, M., Peng, Y., Feng, M., & Liu, G. (2023). Backscatter communication meets practical battery-free Internet of Things: A survey and outlook. *IEEE Communications Surveys & Tutorials*, 25(3), 2021-2051.
- [4] Liu, V., Parks, A., Talla, V., Gollakota, S., Wetherall, D., & Smith, J. R. (2013). Ambient backscatter: Wireless communication out of thin air. *ACM SIGCOMM computer communication review*, 43(4), 39-50.
- [5] Kellogg, B., Parks, A., Gollakota, S., Smith, J. R., & Wetherall, D. (2014, August). Wi-Fi backscatter: Internet connectivity for RF-powered devices. In *Proceedings of the 2014 ACM Conference on SIGCOMM* (pp. 607-618).
- [6] Zhang, P., Bharadia, D., Joshi, K., & Katti, S. (2016, November). Hitchhike: Practical backscatter using commodity wifi. In *Proceedings of the 14th ACM conference on embedded network sensor systems CD-ROM* (pp. 259-271).
- [7] Bharadia, D., Joshi, K. R., Kotaru, M., & Katti, S. (2015). Backfi: High throughput wifi backscatter. *ACM SIGCOMM Computer Communication Review*, 45(4), 283-296.
- [8] Zhang, P., Josephson, C., Bharadia, D., & Katti, S. (2017, November). Freerider: Backscatter communication using commodity radios. In *Proceedings of the 13th international conference on emerging networking experiments and technologies* (pp. 389-401).
- [9] Zhao, Jia, Wei Gong, and Jiangchuan Liu. "X-tandem: Towards multi-hop backscatter communication with commodity wifi." *Proceedings of the 24th annual international conference on mobile computing and networking*. 2018.
- [10] Iyer, V., Talla, V., Kellogg, B., Gollakota, S., & Smith, J. (2016, August). Inter-technology backscatter: Towards internet connectivity for implanted devices. In *Proceedings of the 2016 ACM SIGCOMM Conference* (pp. 356-369).
- [11] Talla, V., Hesar, M., Kellogg, B., Najafi, A., Smith, J. R., & Gollakota, S. (2017). Lora backscatter: Enabling the vision of ubiquitous connectivity. *Proceedings of the ACM on interactive, mobile, wearable and ubiquitous technologies*, 1(3), 1-24.
- [12] Hesar, Mehrdad, Ali Najafi, and Shyamnath Gollakota. "{NetScatter}: Enabling {Large-Scale} Backscatter Networks." In *16th USENIX symposium on networked systems design and implementation (NSDI 19)*, pp. 271-284. 2019.
- [13] Peng, Y., Shangguan, L., Hu, Y., Qian, Y., Lin, X., Chen, X., ... & Jamieson, K. (2018, August). PLoRa: A passive long-range data network from ambient LoRa transmissions. In *Proceedings of the 2018 conference of the ACM special interest group on data communication* (pp. 147-160).
- [14] Wang, Anran, Vikram Iyer, Vamsi Talla, Joshua R. Smith, and Shyamnath Gollakota. "{FM} backscatter: Enabling connected cities and smart fabrics." In *14th USENIX Symposium on Networked Systems Design and Implementation (NSDI 17)*, pp. 243-258. 2017.
- [15] D. -T. Phan-Huy, D. Barthel, P. Ratajczak, R. Fara, M. d. Renzo and J. de Rosny, "Ambient Backscatter Communications in Mobile Networks: Crowd-Detectable Zero-Energy-Devices," in *IEEE Journal of Radio Frequency Identification*, vol. 6, pp. 660-670, 2022.
- [16] Liao, J., Wang, X., Ruttik, K., Jantti, R., & Dinh-Thuy, P. H. (2023). Ambient FSK Backscatter Communications using LTE Cell Specific Reference Signals. *arXiv preprint arXiv:2301.13664*.
- [17] Liao, J., Ruttik, K., Jantti, R., & Dinh-Thuy, P. H. (2024). Coded Backscattering Communication with LTE Pilots as Ambient Signal. *arXiv preprint arXiv:2402.12657*.
- [18] Yang, Shanglin, Yohann Bénédic, Dinh-Thuy Phan-Huy, Jean-Marie Gorce, and Guillaume Villemaud. "Indoor Localization of Smartphones Thanks to Zero-Energy-Devices Beacons." In *2024 18th European Conference on Antennas and Propagation (EuCAP)*, pp. 1-5. IEEE, 2024.
- [19] 3GPP TR 38.848 v18.0.0 "Study on Ambient IoT (Internet of Things) in RAN" [online link](#). 2023-09-29.
- [20] 3GPP TR 22.840 v19.0.0 "Study on Ambient power-enabled Internet of Things" [online link](#). 2023-12-22.
- [21] 3GPP TR 38.769 v2.0.0 "Study on solutions for Ambient IoT (Internet of Things) in NR" [online link](#). 2024-12-04.
- [22] 3GPP TS 36.331 "Radio Resource Control (RRC); Protocol specification" [online link](#). 2024-09-27.
- [23] srsRAN opensource project, <https://www.srsrte.com/>.
- [24] SHAQIRI, Mirlinda, Teuta ILJAZI, Lazim KAMBERI, and Rushadije RAMANI-HALILI. "Differences Between The Correlation Coefficients Pearson, Kendall And Spearman." *Journal of Natural Sciences and Mathematics of UT 8*, no. 15-16 (2023): 392-397.
- [25] Xu, F., Hussain, T., Ahmed, M., Ali, K., Mirza, M. A., Khan, W. U., ... & Han, Z. (2023). The state of AI-empowered backscatter communications: A comprehensive survey. *IEEE Internet of Things Journal*.



> REPLACE THIS LINE WITH YOUR MANUSCRIPT ID NUMBER (DOUBLE-CLICK HERE TO EDIT) <

**Ahmed EISanhoury**, Ahmed has over than two decades of experience in wireless systems and product design. As a lead of IoT Engineering, he has served joint industry-academic activities during his career, strengthening the link between academic research and practical industry needs. On academic side, after obtaining his B.Sc. and M.Sc. from Cairo University in 1998 and 2006, respectively, he currently pursues his PhD degree in electronics & communications engineering from Cairo University. He published several times in IEEE conferences, presented his work in-person overseas in Morocco, Malaysia, and France. Also, he became informa certified with Distinction grade from informa & Derby University in LTE and Advanced Communications. On industry side, he is designated as Orange Expert, joined Orange Experts community since 2020 till present.

**Islam Galal**, Islam received his BS degree in Electronics and Communications Engineering from the Benha Faculty of Engineering, Benha University (BU), Egypt, in 2008. He earned his MS degree in Communications and Computer Engineering from the Faculty of Engineering, BU, in 2013. Previously, he was an Assistant Lecturer at the Faculty of Engineering, BU. Currently, he is a Principal Embedded Engineer with the IoT and Networks Division at Orange Innovation Egypt, where he oversees firmware architecture, development, and integration for advanced embedded systems and IoT solutions. His research and technical interests include software-defined radio, machine-to-machine communication, digital communication transceivers, low-power embedded systems, and IoT architectures.

**Khaled AlKady**, Khaled Alkady obtained his B.Sc. in Computer Science in 2005 from the Faculty of Computers and Information at Cairo University - Egypt. He later transitioned to the field of robotics and autonomous navigation systems, completing his M.Sc. in Autonomous Systems in 2019 at H-BRS University of Applied Sciences - Germany. Currently, he leads the Edge-AI and Embedded Systems unit at the Orange Innovation Center in Cairo. His work in Edge-AI focuses on designing and optimizing deep learning solutions for edge devices with limited computational capabilities. The activities on the Embedded Systems side covers building ultra-low-power IoT solutions, power-line communication systems, mobile ad hoc networks, and algorithms for ambient backscattering communication in 4G networks.

**Amal Elkhodary**, Amal received her Bachelor's degree in engineering from the Faculty of Engineering, Suez Canal University, in 2021. After graduation, she completed the 9-month Wireless Communication Track program at the Information Technology Institute (ITI), Egypt. In 2023, she joined Orange Innovation, Egypt, where she has been engaged in research and development, focusing on backscattering tags and their application within 4G wireless communication systems. Her research interests include embedded systems, digital signal processing, and advancements in wireless communication technologies.

**Ayman M. Hassan**, Obtained his B.Sc. in Telecommunications Engineering from Benha High Institute of Technology, Egypt in 1993. He worked towards his M.Sc. and Ph.D. degrees in Spread Spectrum communications from Cairo University in 1998, and 2002, resp. He is now heading the IoT and Networks team at Orange Innovation Center in Cairo, which is responsible for design, deployment and deployment of Proof of Concepts for Telecom Solutions in AMEA countries. IoT solutions of interest include: Utility Metering, Ultra-Low-Power nano-computers, and LORA-based IoT solutions. Research interests include Power Line Communication, Spread Spectrum, Ad-Hoc Networks, Backscattering and Military Communications. He is working also as an associate professor at Benha University and as an Adjunct Faculty at the American University in Cairo.

**Dinh-Thuy Phan-Huy**, [SM] received her degree in engineering from Supelec in 2001 and her Ph.D. degree in electronics and telecommunications from the National Institute of Applied Sciences (INSA) of Rennes, France, in 2015. In 2001, she joined France Telecom R&D (now Orange Innovation), France, where she currently works as a research project manager. Her current research interests include wireless communications and 6G. She is an Orange Fellow.